SYNTHESIS OF SMALL CRYSTALS ZEOLITE NaA BY A TWO-STEP GROWTH APPROACH

X. ZHANG [a*], C. CHEN[a], R. YANG [b]
[a]*College of Chemistry and Chemical Engineering, Xuchang University, Xuchang, 461000, China*
[b]*College of Biological and Chemical Engineering, Anhui Polytechnic University, Wuhu 241000, China*

Small crystals zeolite NaA were hydrothermally synthesized with a two-step variable-temperature approach, where the hydrogel was first treated at low temperature (283 K) for various times, followed conducted at high temperature (333 K) for 36 h. The products were characterized by XRD, FTIR, SEM and particle size analysis technique. The results indicated that the samples synthesized by a two-step hydrothermal crystallization procedure had smaller particle sizes and narrower particle size distributions than that by an isothermal program. The reasons may be due to that the low temperature at the initial stage was beneficial to the fast nucleation of zeolite NaA with negligible crystal growth, while the crystal growth was dominant at the second stage. Moreover, no peak of other phase or amorphous material was detected in the end samples.

(Received September 24, 2016; Accepted November 26, 2016)

Keywords: Zeolite NaA, Crystallization, Two-step, Crystal size

1. Introduction

Zeolites are porous crystalline aluminosilicates of SiO_4^{4-} and AlO_4^{5-} tetrahedra connected by oxygen bridges [1,2]. The sizes and shapes of the micropores, and the cavities, are determined exclusively by the crystal structure of the zeolite. Out of various low silica zeolites, zeolite NaA is one of the microporous crystalline aluminosilicate zeolites which has a channel opening size of 0.4 nm, the small pore size of NaA zeolite makes the separation of small molecules by difference in size possible [3]. Furthermore, the pore of zeolite NaA can be modified to 5A or 3A by ion exchange with aqueous solutions of calcium or potassium salts [4]. Because of its adsorption, ion exchange and porosity properties, zeolite NaA is widely applied in various applications such as household products [5], aquaculture [6] and petrochemical-related industry [7].

Due to unique applications of zeolite NaA, various works have been aimed at the synthesis of this kind of zeolite by different methods. Sathupunya et al. [8] have reported the synthesis of zeolite NaA from alumatrane and silatrane by sol–gel microwave techniques. Ju et al. [9] synthesized zeolite NaA in a microchannel reactor, they found that the required crystallization time with close crystallinity in the reactor was remarkably decreased compared to that needed in the batch system, which resulted from fast heat transfer and auto-creation segmented flow of the synthesis solution in the reactor. In addition, Mohamed et al. [10] recommended that the suitable conditions for the synthesis were SiO_2:Al_2O_3:H_2O:Na_2O molar ratios=1:0.83:150:1.15, well-shaped crystals were obtained at 110 ◦C with 20 days crystallization time. Similar effect was observed by Ismail et al [11]. In a more detail study, they revealed that the zeolites were formed only with sodium aluminate as aluminum source and fumed silica, colloidal silica, sodium metasilicate as silica source. The results of numerous investigations gave very quality and worthy

*Corresponding author: zxzx5973428@163.com

data [12–14]. However, from these literatures, zeolites NaA syntheses were performed by a one-step approach, with the particle size distribution ranges of ca. 1–5 um.

Herein, we reported on the synthesis of small crystals zeolite NaA by applying a two-step hydrothermal crystallization procedure, where the hydrogel was first treated at low temperature (283 K) for various times, followed conducted at high temperature (333 K) for 36 h. Moreover, the two-step crystallization mechanism was also proposed.

2. Methods

2.1. Zeolite synthesis

In a typical synthesis, 14.6 g of sodium hydroxide (99%, Merck) was dissolved in 162.5 ml of deionized water, followed by the addition of 2.98 g of sodium aluminate (anhydrous, Sigma-Aldrich) to get solution A. 10.0 g of 30 wt.% aqueous colloidal silica (Ludox HS-30, Sigma–Aldrich) was weighed and slowly poured into the solution A under vigorous stirring, the molar composition of the resultant hydrogel was 4.0 Na_2O:0.35 Al_2O_3:1.0 SiO_2:200 H_2O. The hydrogel was stirred for 30 min and then stored in sealed polypropylene bottles. The crystallization controlled by a two-step variable-temperature process was conducted at 283 K for different periods of 0, 12, 24, 36, 48 or 72 h, subsequently at 333 K for 36 h. After synthesis, the solid products were filtered off, thoroughly washed with deionized water, then dried at 373 K overnight.

2.2. Characterization and Analyses

Powder X-ray diffraction (XRD) patterns were obtained using a Philips APD-3720 diffractometer with Cu Kα radiation, operated at 20 mA and 40 kV. The diffraction patterns were collected in the 2θ range of 5–40° at a scan speed of 0.05° 2θ/min. Transmission IR spectra were recorded by a JASCO Fourier transform infrared (FTIR) spectrometer with a resolution of 4 cm^{-1} using a KBr method. The scanning electron microscopy (SEM) images were taken on a JEOL JSM-6700F microscope equipped with a cold-field emission gun, operating at 2 kV and 10 μA. Particle size distribution curves of the crystalline samples were determined with a Malvern Mastersizer 2000 laser light-scattering particle size analyzer with water used as the medium for dispersion of the zeolite samples. The solution was ultrasonicated for 40 min before the measurement.

3. Results and discussion

Fig. 1 shows XRD patterns of samples obtained by a two-step variable-temperature process conducted at 283 K for different periods of times. As shown in Fig. 1, the synthesis products match the characteristic peaks of zeolite NaA at 2 theta values of 7.2°, 10.3°, 12.6°, 16.2°, 21.8°, 24°, 26.2°, 27.2°, 30°, 30.9°, 31.1°, 32.6°, 33.4° and 34.3° that were reported by Treacy and Higgins[15], suggesting successful synthesis of zeolite NaA with good crystallinity. Moreover, the XRD diffraction peaks of samples obtained with longer crystallization times (48 and 72 h) are relatively broad, implying that the products consist of very small crystals.

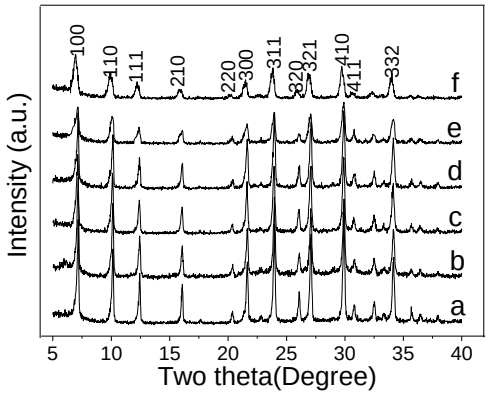

Fig. 1. XRD patterns of samples obtained at 283 K for different periods of times. (a) 0 h, (b) 12 h, (c) 24 h, (d) 36 h, (e) 48 h, and (f) 72 h.

The FTIR spectra of samples are shown in Fig. 2. As a result, the characteristic band at 557 cm^{-1} ascribed to the external vibration of double four-rings of zeolite NaA framework, 1001 cm^{-1} for the internal vibration of (Si, Al)–O asymmetric stretching, 671 cm^{-1} for the internal vibration of (Si, Al)–O symmetric stretching and 467 cm^{-1} due to the internal vibration of (Si, Al)–O bending are observed. The band related to OH also appear at about 1655 cm^{-1} [16,17]. These results are in good agreement with the XRD results.

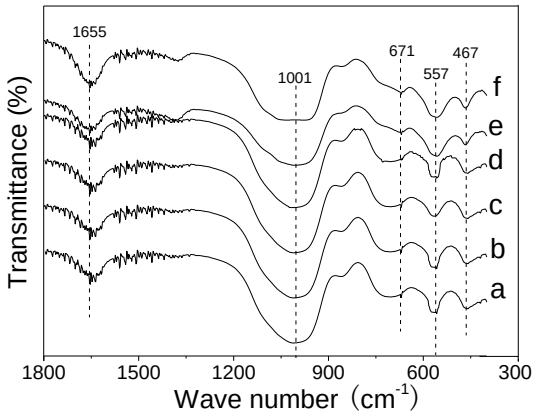

Fig. 2. FTIR spectra of samples obtained at 283 K for different periods of times. (a) 0 h, (b) 12 h, (c) 24 h, (d) 36 h, (e) 48 h, and (f) 72 h.

The SEM micrographs and corresponding particle size distributions of samples are shown in Fig. 3 and Fig. 4, respectively. From Fig. 3, the zeolite NaA crystallites exhibit a shape of edge-truncated cubes (rhombic dodecahedra) with edge lengths ca. 1 um, while the {110} faces are observable (Fig. 3a). The samples obtained with long crystallization times at low temperature stage show smaller particle sizes (Fig. 3b-f), as expected. It can also be observed that beside single crystals, many particles are intergrown from two or more cubes. The longer the crystallization time at low temperature, the smaller the particle size and the more the intergrowth will be. As shown in Fig. 4, the samples synthesized with the crystallization times of 0, 12, 24, 36, 48, and 72 h show the average particle sizes of 916, 697, 412, 327, 234 and 229 nm, and the particle size distribution ranges of 610–1230, 504–920, 265–560, 201–460, 148–376 and 145–370 nm, respectively.

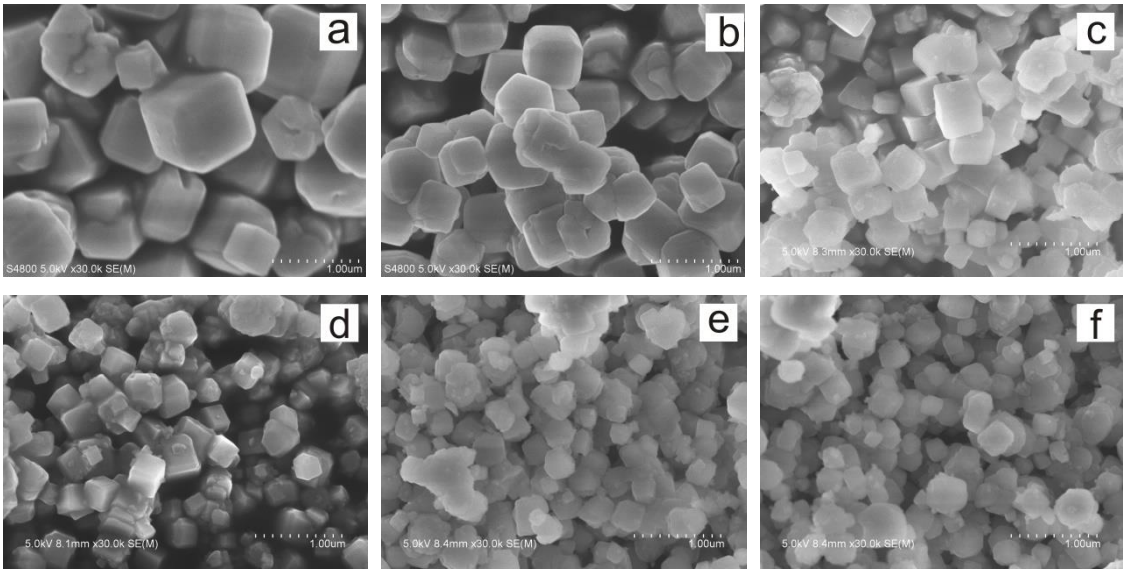

Fig. 3. SEM pictures of samples obtained at 283 K for different periods of times. (a) 0 h, (b) 12 h, (c) 24 h, (d) 36 h, (e) 48 h, and (f) 72 h.

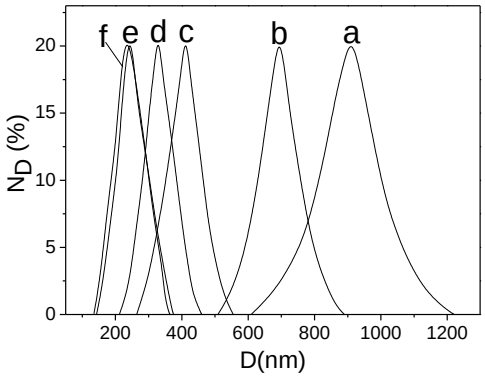

Fig. 4. Particle size distribution curves of samples obtained at 283 K for different periods of times. (a) 0 h, (b) 12 h, (c) 24 h, (d) 36 h, (e) 48 h, and (f) 72 h. N_D is number percentage of crystals having the spherical equivalent diameter D.

From the above results, the samples synthesized by a two-step variable-temperature process show smaller particle sizes and narrower particle size distributions than that by an isothermal program. Generally speaking, the energy for nuclei formation (ca. 15 kJ/mol) is less than the energy for crystal growth (ca. 60 kJ/mol) [18]. For the two-step zeolite syntheses, we assume that the low temperature at the initial stage is beneficial to the fast nucleation of zeolite NaA with negligible crystal growth, while the subsequent high temperature is favorable for the crystal growth [19,20]. Therefore, the fast nucleation at the initial stage may allow the formation of a large quantity of crystal nuclei, which provides a favorable option for the following crystallization stage. Also, Sun et al [21]. have pointed that longer time of low temperature crystallization led to the isolation of the Al-rich region by further incorporation of Si into precipitate, which gave rise to a larger number of smaller nuclei and resulted in a higher final yield of product. By contrast, crystal growth is dominant at high temperature, and the second synthesis temperature controls only the linear growth rate of the crystals. On the other hand, Caballero et al. [22] reported that too short time of low temperature crystallization would lead to the occurrence of undesired nucleation of the competing phase. While in our case, no peak of other phase or amorphous material is detected in the end samples.

4. Conclusions

In summary, the samples synthesized by a two-step variable-temperature process showed smaller particle sizes and narrower particle size distributions than that by an isothermal program. The reasons may be due to that the low temperature at the initial stage was beneficial to the fast nucleation of zeolite NaA with negligible crystal growth, while the crystal growth was dominant at elevated temperature. The enhancement of crystallization time at low temperature allowed more uniform nucleation to occur through the gel matrix, which assisted the formation of zeolite crystals with small sizes and narrow size distributions at the second stage.

Acknowledgments

This work was supported by the College Natural Science Foundation of Henan Province (17B530004) and the National Nature Science Foundation of China (51572004).

References

[1] A. Dyer, An Introduction to Zeolite Molecular Sieve, John Wiley, London, 1988.
[2] R.M. Barrer, Zeolites and Clay Minerals as Sorbents and Molecular Sieves, Academic Press, London, 1978.
[3] B. Bayati, A.A. Babaluo, R. Karimi, J. Eur. Ceram. Soc. **28**, 2653 (2008).
[4] Z. Gao, L.V.C. Rees, Zeolites **2**, 72 (1982).
[5] K. C. Khulbe, T. Matsuura, C. Y. Feng, A. F. Ismail, RSC Adv. **6**, 42943 (2016).
[6] B. Biškup, B. Subotić, Sep. Purif. Technol. **37**, 17 (2004).
[7] D. Liu, Y. Zhang, J. Jiang, X. Wang, C. Zhang, X. Gu, RSC Adv. **5**, 95866 (2015).
[8] M. Sathupunya, E. Gulari, S. Wonghasemjit, J. Eur. Ceram. Soc. **23**, 1293 (2003).
[9] J.X. Ju, C.F. Zeng, L.X. Zhang, N.P. Xu, Chem. Eng. J. **116**, 115 (2006).
[10] R.M. Mohamed, A.A. Ismail, G. Kini, I.A. Ibrahim, B. Koopman, Colloid. Surface. A **348**, 87 (2009).
[11] A.A. Ismail, R.M. Mohamed, I.A. Ibrahim, G. Kini, B. Koopman, Colloid. Surface. A **366**, 80 (2010).
[12] X. Liu, Y. Wang, X. Cui, Y. He, J. Mao, Powder Technol. **243**, 184 (2013).
[13] T. Qian, J. Li, Adv. Powder Technol. **26**, 98 (2015).
[14] S. Bohra, D. Kundu, M.K. Naskar, Ceram. Int. **40**, 1229 (2014).
[15] M.J. Treacy, J.B. Higgins, Collection of simulated XRD powder patterns for zeolites, fourth ed., Elsevier, Amsterdam, The Netherlands, 2001.
[16] F. Fotovat, H. Kazemian, M. Kazemeini, Mater. Res. Bull. **44**, 913 (2009).
[17] M. Alkan, C. Hopa, Z. Yilmaz, H. Guler, Micropor. Mesopor. Mat. **86**, 176 (2005).
[18] T. Brar, P. France, P.G. Smirniotis, Ind. Eng. Chem. Res. **40**, 1133 (2001).
[19] S. Sang, Z. Liu, P. Tian, Z. Liu, L. Qu, Y. Zhang, Mater. Lett. **60**, 1131 (2006).
[20] J. Shao, Q. Ge, L. Shan, Z. Wang, Y. Yan, Ind. Eng. Chem. Res. **50**, 9718 (2011).
[21] G. Sun, Y. Liu, J. Yang, J. Wang, J. Porous Mat. **18**, 465 (2011).
[22] I. Caballero, F.G. Colina, J. Costa, Ind. Eng. Chem. Res. **46**, 1029 (2007).